Multistep Brownian Dynamics: Application to Short Wormlike Chains

S. A. ALLISON and J. A. McCAMMON, *Department of Chemistry, University of Houston Central Campus, Houston, Texas 77004*

Synopsis

Brownian dynamics simulations of short wormlike chains are carried out using the method of Ermak and McCammon [(1978) *J. Chem. Phys.* **69,** 1352–1360]. Following Hagerman and Zimm [(1981) *Biopolymers* **20,** 1481–1502], the wormlike chain is modeled as a string of beads. In each simulation, the dynamic evolution of an ensemble of 100 randomly generated chains is calculated for a period of from 3 to 200 ns. Two different "experiments," fluorescence depolarization and dynamic light scattering, were performed in these simulations. Since we are primarily interested in the bending motions and not the torsional motions in this work, we have placed the transition moments along the local symmetry axis of the wormlike chain in the fluorescence depolarization "experiment." As predicted by the Barkley and Zimm theory [(1979) *J. Chem. Phys.* **70,** 2991–3008], a considerable amount of rapid bending motion was detected by fluorescence depolarization, though not as much as predicted by theory. We conclude that these differences are primarily due to differences between the model used in the theory and the simulations. The light-scattering experiment was found to be insensitive to internal motion in the low scattering angle limit.

INTRODUCTION

In recent years, the continued development of relaxation techniques such as fluorescence depolarization, dynamic light scattering, flow and electric birefringence and dichroism, and nmr has greatly increased our understanding of the dynamic and conformational features of biological macromolecules in solution. Although internal flexibility in chain molecules such as DNA has been recognized for many years now,[1] flexibility in macromolecules such as myosin,[2,3] tRNA,[4] immunoglobulins,[5–8] L-arabinose binding protein,[9] and lysozyme[10] represent more recent discoveries. This structural flexibility, in turn, can be expected to be associated with the function of specific biopolymers in many cases.

Parallel developments in the hydrodynamic theory of rigid,[11–15] and flexible[16–23] macromolecules have facilitated the interpretation of these results on the basis of molecular models. The hydrodynamic theories of rigid structures and the connection between the transport properties derived from them and experimental observables have been established. For flexible macromolecules, the problem is more complicated, although a number of specific models have been treated. Zero and Pecora[24] have recently studied depolarized light scattering from a small, once-broken rod.

Biopolymers, Vol. 23, 363–375 (1984)

CCC 0006-3525/84/020363-13$04.00

Their analytic treatment is apparently exact in the limit of a linear once-broken rod. Harvey and Cheung[17] used Brownian dynamics to simulate the fluorescence depolarization from hinged macromolecules. Subsequently, Wegener[21] was able to relate transport coefficients of a totally flexible array of cylindrically symmetric subunits to experimental observables. In both of these studies, however, it was assumed that hydrodynamic interaction between subunits could be neglected. This hydrodynamic interaction is now known to be significant.[18,22,23]

For flexible macromolecules, the most highly developed hydrodynamic theories are of very flexible Gaussian or Rouse-Zimm chains pioneered by Kirkwood[25] and Zimm.[26] The connections of these theories to observables such as intrinsic viscosity,[25,26] sedimentation,[25,26] flow dichroism,[27,28] and dynamic light scattering[29-31] are well established. In virtually all pre-1980 theories, however, fluctuations in the hydrodynamic interaction between subunits were ignored. Recent computer simulations initiated by Zimm[32] have shown that this preaveraging approximation leads to errors even though their magnitude is still disputed.[32-35] In addition to the Gaussian chain, dynamic theories of wormlike[36-39] and helical wormlike chains[40-42] have appeared. In order to obtain tractable results, it has been necessary to make certain approximations. Since mathematical rather than physical reasons have made it necessary to make these approximations, it is difficult to assess the errors they produce. The history of the preaveraging approximation in Gaussian chain dynamics is a perfect example of this.

In this study, we use the method of Brownian dynamics to simulate fluorescence depolarization and dynamic light scattering from short wormlike chains. We chose this system since it is of intermediate complexity and can be compared to the analytic theory of Barkley and Zimm.[39] We would like to emphasize, however, that the methods we use are applicable to a far broader class of molecular models than Gaussian or wormlike chains.[23]

Computer simulations of local motions in chain molecules in a solvent bath have proliferated in the last few years. The advantage of Brownian dynamics,[34,35,43-51] based on diffusion or Langevin equations, over molecular dynamics,[52-57] which is based on classical equations of motion, is that much longer simulation times are possible ($\sim 10^{-6}$ vs $\sim 10^{-10}$ s).[51] This advantage is obtained at the cost of using a simplified model to characterize the interaction of the solvent with the macromolecule and ignoring the detailed history of the solvent. Since we are primarily interested here in the comparatively slow motions of large semiflexible macromolecules and relating these to experimental observables, Brownian dynamics appeared to be an ideal method.

Using Brownian dynamics to simulate the motion of a many body structure accurately is complicated by two factors. First, the stochastic solvent forces depend on the instantaneous configuration of the subunits comprising the macromolecule.[23,58] Second, subunit displacements that result from forces of constraint are complicated by hydrodynamic inter-

actions between subunits.[23,59] In this work, we account for both of these factors.

WORMLIKE CHAIN MODEL

Following Hagerman and Zimm,[60] the wormlike chain (wlc) is modeled as a string of N touching beads of radius a linked end-to-end by $N-1$ bonds. In order to mimic the hydrodynamic behavior of a continuous wlc cylinder with radius $b = 13$ Å (corresponding to DNA), a bead radius of $a = 15.9$ Å $\simeq (3/2)^{1/2}b$ was used, as in Ref. 60. This insures that the volumes of the bead model and the corresponding continuous wlc (with length $L = 4Na^3/3b^2$) are equal. As discussed elsewhere,[60] the diffusion constants of the volume-adjusted bead and cylinder models agree to within a few percent.

Initial configurations were randomly generated using the algorithm of Hagerman and Zimm.[60] To check the chain-generation procedure, computed values of $\langle h^2\rangle/L^2$ (reduced mean-squared end-to-end distance) for ensembles of chains were compared with those predicted by[1,60]

$$\langle h^2\rangle/L^2 = (2P/L)[1 - P/L + (P/L)\exp(-L/P)] \tag{1}$$

where P is the persistence length. Good agreement ($\lesssim 2\%$) was achieved for ensembles of 100 chains or more over a broad range of L and P values. All subsequent dynamics simulations were carried out on 100 chains prepared in this way.

The bending forces acting on the subunits, which are needed in the dynamics simulations, were obtained using the model of Harris and Hearst.[36] Let F_{x_i} denote the x-component of the force acting on subunit i, and x_i its x position; then,

$$F_{x_i} = \begin{cases} -g(x_i - 2x_{i\pm1} + x_{i\pm2}), & i = 1(+), n(-) \\ -g(-2x_{i\mp1} + 5x_i - 4x_{i\pm1} + x_{i\pm2}), & i = 2(\text{upper sign}),\ N-1(\text{lower sign}) \\ -g(x_{i-2} - 4x_{i-1} + 6x_i - 4x_{i+1} + x_{i+2}) & 3 \le i \le N-2 \end{cases} \tag{2}$$

where $g = Pk_BT/(2a)^3$ is the bending force constant.[1]

DYNAMICS

In order to simulate the Brownian diffusion of a system of N identical interacting spheres, the method of Ermak and McCammon is used.[58] If the initial position of subunit i is $\mathbf{r}_i^0$, its position after a dynamics time step, Δt, is given by

$$\mathbf{r}_i' = \mathbf{r}_i^0 + \frac{\Delta t}{k_BT}\sum_{j=1}^{N} \mathbf{D}_{ij}^0 \cdot \mathbf{F}_j^0 + \mathbf{R}_i(\Delta t) \tag{3}$$

where k_B is Boltzmann's constant, T is the absolute temperature, $\mathbf{F}_j^0$ is the initial force acting on subunit j excluding forces of constraint, $\mathbf{R}_i$ is a vector of Gaussian random numbers of zero mean and variance–covariance

$$\langle \mathbf{R}_i \mathbf{R}_j \rangle = 2\mathbf{D}_{ij}^0 \Delta t \tag{4}$$

and $\mathbf{D}_{ij}^0$ is the initial hydrodynamic interaction tensor between subunits i and j. The modified Oseen tensor with stick boundary conditions was used to approximate $\mathbf{D}_{ij}^0$. For identical, nonoverlapping beads of radius a, it is given by[61,62]

$$\begin{aligned}\mathbf{D}_{ij} &= \frac{k_B T}{6\pi\eta a}\mathbf{I}\delta_{ij}, \quad i = j \\ &= \frac{k_B T}{8\pi\eta r_{ij}}\left\{\left(\mathbf{I} + \frac{\mathbf{r}_{ij}\mathbf{r}_{ij}}{r_{ij}^2}\right) + \frac{2a^2}{r_{ij}^2}\left(\tfrac{1}{3}\mathbf{I} - \frac{\mathbf{r}_{ij}\mathbf{r}_{ij}}{r_{ij}^2}\right)\right\}, \quad i \neq j\end{aligned} \tag{5}$$

where δ_{ij} is the Kronecker delta, $\mathbf{I}$ is the 3×3 identity matrix, and $\mathbf{r}_{ij}\mathbf{r}_{ij}$ denotes the 3×3 dyad corresponding to the displacement vector between subunits i and j. The $\mathbf{R}_i$ vector in Eq. (3) represents the stochastic displacement of subunit i due to collision with the solvent and is given explicitly elsewhere.[23,58] Each component of $\mathbf{R}_i$ consists of a linear combination of $3N$ normally distributed Gaussian random numbers ($\langle x_m \rangle = 0$, $\langle x_m x_n \rangle = 2\delta_{mn}\Delta t$) obtained from random-number generator GGNSM from the IMSL subroutine library.[63]

Because of forces of constraint between subunits, the coordinates, $\{\mathbf{r}_i'\}$, must be corrected. In the present study, the SHAKE-HI algorithm, described in detail elsewhere,[23] is used to enforce the constraints. For the wlc model, there are $N - 1$ constraints that fix the distance between adjacent subunits at $2a$. Enforcing the pth constraint, displacement correction vectors are added to each subunit:

$$\delta\mathbf{r}_i = \mathbf{H}_{ip}^0\{4a^2 - (\mathbf{r}'_{p+1,p})^2\} \tag{6}$$

where $\mathbf{r}'_{p+1,p} = \mathbf{r}'_{p+1} - \mathbf{r}'_p$ and the prime signifies the coordinates just prior to the enforcement of the pth constraint, and

$$\mathbf{H}_{ip}^0 = \frac{(\mathbf{D}_{i,p+1}^0 - \mathbf{D}_{ip}^0)\cdot\mathbf{r}_{p+1,p}^0}{4\mathbf{r}_{p+1,p}^0\cdot(\mathbf{D}_{pp}^0 - \mathbf{D}_{p+1,p}^0)\cdot\mathbf{r}_{p+1,p}^0} \tag{7}$$

Since the enforcement of the pth constraint partially destroys those that were enforced previously, it is necessary to repeat the procedure of enforcing all constraints until they are satisfied to within a specified tolerance level (10^{-3} Å in this work). The effectiveness of the SHAKE-HI algorithm has been demonstrated elsewhere[23] and is similar to the constraint algorithm of Fixman and Kovac.[59]

SIMULATIONS

Between 200 and 600 steps of Brownian dynamics with a time step between 10 and 400 ps were carried out on an ensemble of 100 randomly

generated chains. At regular intervals (10 dynamics steps in this work), the $3N$ coordinates were recorded for subsequent analysis. All averages were derived from this data set. The "experiments" we report are only two examples. Many others could be obtained from the same data set. The first "experiment" was fluorescence depolarization from a chromophore with both absorption and emission dipoles lying along the local backbone (parallel to the symmetry axis) of a wlc. The polarization anisotropy is given by[64,65]

$$\begin{aligned} r(t) &= 0.4\langle P_2\{\hat{u}(0)\cdot\hat{u}(t)\}\rangle \\ &= 0.4\exp[-3\langle\theta^2(t)\rangle/2] \end{aligned} \tag{8}$$

where P_2 is a Legendre polynomial, $\hat{u}(t)$ is a unit vector along a particular bond of the wlc at time t, and $\langle\theta^2(t)\rangle$ denotes the mean-square angular displacement of that unit vector. The second experiment was polarized dynamic light scattering, where the important average is the dynamic structure factor, $S(q,t)$, defined by[66]

$$S(q,t) = \frac{1}{N^2}\left\langle \sum_{j,k} \exp(-i\mathbf{q}\cdot\{\mathbf{r}_j(t) - \mathbf{r}_i(0)\})\right\rangle \tag{9}$$

where $\mathbf{q}$ is the scattering vector with magnitude equal to $(4\pi n/\lambda)\sin(\theta/2)$, n is the refractive index, λ is the wavelength of the monochromatic light source, and θ is the scattering angle. The double sum is over all subunits comprising the wlc. For the 10-subunit wlc considered in this work and visible light sources, $qL < 1$, and Eq. (9) simplifies to

$$S(q,t) \simeq 1 - \frac{q^2L^2}{6}G(t) + O(q^4L^4) \tag{10}$$

where

$$G(t) = \frac{1}{N^2L^2}\left\langle \sum_{j,k} \{\mathbf{r}_j(t) - \mathbf{r}_k(0)\}^2\right\rangle \tag{11}$$

Thus, by simulating $G(t)$, $S(q,t)$ can be readily constructed.

RESULTS

In order to test the dynamics program, we first considered a wlc of 10 subunits (L = 317.1 Å) with a persistence length, P, of 10,000 Å to mimic a rigid rod. The results of the fluorescence depolarization simulation are shown in Fig. 1. Except for very short times, the curve increases linearly with time as expected for a rigid rod. The rotational diffusion constant extracted from this curve is $2.72 \times 10^5\ s^{-1}$, which is in good agreement with the value of $2.49 \times 10^5\ s^{-1}$ obtained from the formula of Nakajima and Wada[13] for a rigid linear array of 10 beads. The short time behavior can be attributed to the fact that the structure is not perfectly rigid. Figure 1 represents the depolarization of the central three bonds. For bonds near the end, a greater depolarization was observed; this would not have occurred

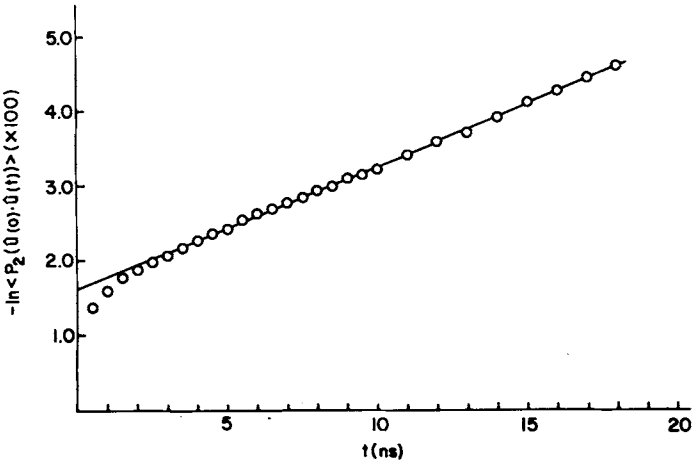

Fig. 1. Fluorescence depolarization simulation of a nearly rigid rod: P = 10,000 Å, L = 317.1 Å, Δt = 50 ps. The transition moments lie along the symmetry axis of the rod.

if the wlc were perfectly rigid. Figure 1 can be understood by considering the simplified model of a "bond" at the end of an otherwise rigid rod structure. The bond is harmonically bound to the rest of the structure and the minimum potential energy corresponds to the bond being collinear with the rest of the structure. The bond can then undergo rotational displacement as a result of flexing as well as overall rotation of the rod. Let $\theta(t)$ represent the net angular displacement perpendicular to the rod axis; then we can write[67]

$$\begin{aligned}\langle\theta^2(t)\rangle &= \langle\theta_r^2(t)\rangle + \langle\theta_f^2(t)\rangle \\ &= 4D^R t + (4a/P)[1 - \exp(-t/\tau)]\end{aligned} \tag{12}$$

where r and f subscripts refer to rotation due to rigid body and flexing displacements, respectively, D^R is the rigid-body diffusion constant, and

TABLE I
End Effects on Fluorescence Depolarization[a]

Bond	$-\ln\langle P_2[\hat{u}(0)\cdot\hat{u}(t)]\rangle$	
	t = 5 ns	t = 20 ns
1 (end)	0.224	0.464
2	0.143	0.287
3	0.134	0.227
4	0.134	0.220
5 (center)	0.137	0.219
6	0.141	0.211
7	0.136	0.230
8	0.149	0.302
9 (end)	0.233	0.478

[a] P = 600 Å, L = 317.1 Å, Δt = 0.1 ns.

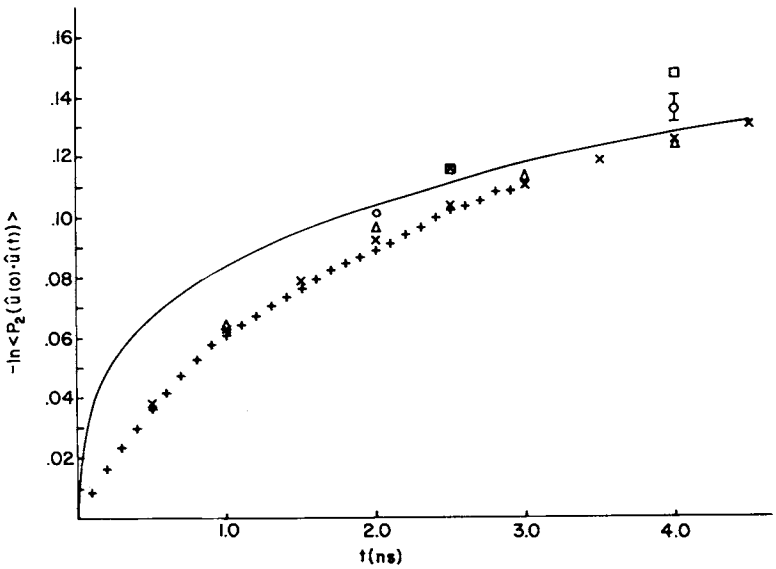

Fig. 2. Short-time fluorescence depolarization of a short wormlike chain: P = 600 Å, L = 317.1 Å, Δt (ps) = 10, +; 50, ×; 100, Δ; 200, ○; 250, ⊠; 400, □. The solid curve is the prediction of the Barkley-Zimm theory (Ref. 39). The transition moments lie along the local symmetry axis of the wlc.

τ is a rapid relaxation time due to flexing. The similarity between this equation and Fig. 1 is obvious.

A more thorough study of a 10-subunit wlc with P = 600 Å was then carried out. As in the case of the "almost rigid rod," bonds near the end of the chain undergo enhanced rotational motion as summarized in Table I. One important point to note is the fact that end effects fall off rapidly on moving toward the center of the chain. In Figs. 2 and 3, the short- and long-time fluorescence depolarization results are plotted. Since we are primarily interested in the chain interior, the data points in these figures represent averages of the three central bonds. The dynamics time step, Δt, was varied from 10 to 400 ps to see how the results were affected. This is an important practical consideration, since an increase in Δt by a factor of 10 allows a 10-fold increase in the overall time range of the simulation without significantly increasing computer time. From Figs. 2 and 3, it can be seen that spurious rotational motion occurs for long time steps, $\Delta t \gtrsim$ 100 ps. This result is evidently due to the nonconstancy of bending forces for long time steps and places a practical upper time limit of about 100 ns on fluorescence depolarization simulations for this system. Also plotted in Figs. 2 and 3 are the results predicted by the Barkley and Zimm theory.[39] For this long elastic cylinder model, a cylinder radius of 13 Å and a persistence length of 600 Å were used. In the lower portion of Fig. 3, the dashed line represents the behavior expected from a corresponding ensemble of *rigid* wlc's with the same L and P used here. From the work of Hagerman

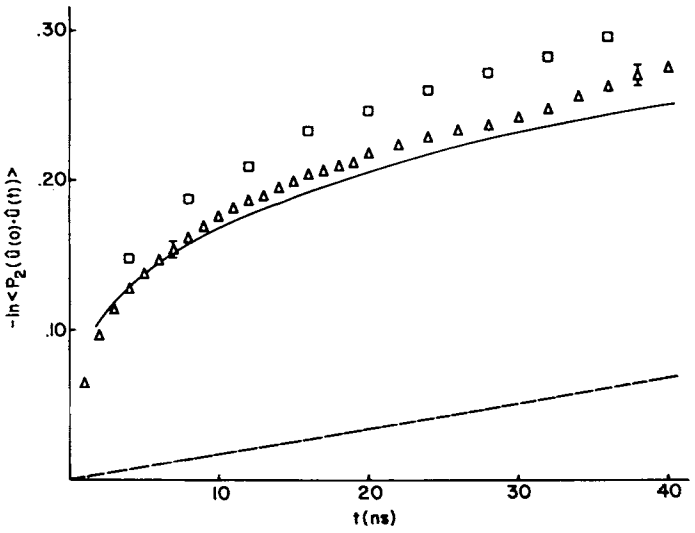

Fig. 3. Same as Fig. 2 but extended out to longer times. The dashed line represents the expected behavior of the corresponding rigid ensemble.

and Zimm,[60] whose wlc model we have adopted, a value of $\langle D^R \rangle = 2.84 \times 10^5\ s^{-1}$ can be obtained. (Brackets denote an ensemble average of the different frozen wlc configurations.) It is evident from these results that the fluorescence depolarization "experiment" reveals a considerable mount of internal motion. Since the Barkley and Zimm theory treats a long flexible cylinder,[39] it is necessary to subtract the overall motion from the simulation if a comparison between the two is to be made. Using the same separation scheme used in Eq. (12), the results are plotted in Fig. 4.

Finally, the relevant average for dynamic light scattering, $G(t)$, is plotted in Fig. 5. Unlike fluorescence depolarization, $G(t)$ is insensitive to the dynamics time step. Note also that it increases linearly, which is the behavior expected of a rigid body. For a rigid body, the dynamic structure factor is given by[66]

$$S(q,t) = S(q,0) \exp(-q^2 D^T t) \tag{13}$$

where D^T is the translational diffusion constant. Combining this result with Eq. (10) and retaining terms to order q^2, it is straightforward to show

$$D^T = \frac{L^2}{6t} [G(t) - G(0)] \tag{14}$$

From the slope of Fig. 5, we obtain $D^T = 3.90 \times 10^{-7}\ cm^2/s$. This can be compared with a value of 4.08×10^{-7} calculated for a continuous wlc.[68] The nonlinearity of Fig. 5 at long t is due to statistical error in the simulations.

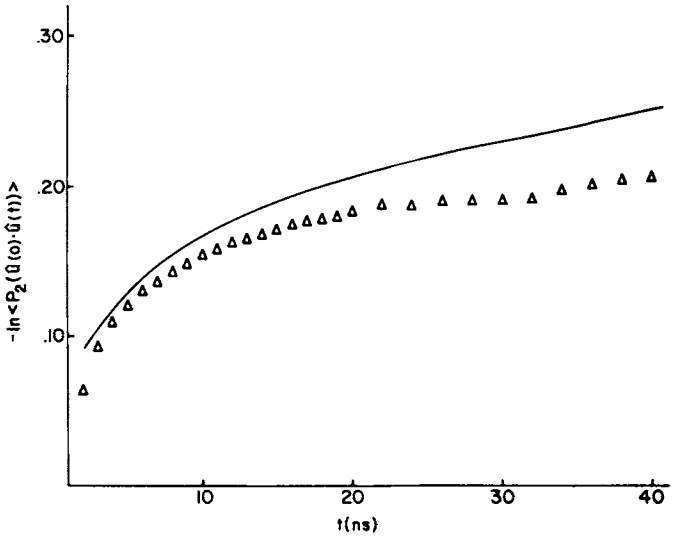

Fig. 4. Same as Figs. 2 and 3, but the simulations have had the contribution of overall rotation subtracted out.

DISCUSSION

The fluorescence depolarization simulations are in good qualitative agreement with the Barkley and Zimm theory[39] even though the latter exhibits more bending motion at short ($t \lesssim 4$ ns) and long ($t \gtrsim 20$ ns) times. Because of obvious differences between the two models, short discrete chain versus long elastic cylinder, perfect agreement cannot be expected. As discussed by Hagerman and Zimm,[60] however, the overall hydrodynamic properties of the two models should be nearly identical. End effects in the simulations are probably small in light of the results given in Table I. Since they lead to enhanced rotational motion, the simulation results plotted in Figs. 2 and 3 might be regarded as upper bounds on the bending motion that could be expected for the interior of a long chain. However, the long elastic cylinder model allows for bending motions that are not present in the short discrete chain model at both very short and long times. For the elastic cylinder, the relaxation time of a bending mode with a quarter wavelength of 17 Å is about 0.1 ns.[39] Since this corresponds closely to the bead size used in this work, much of the short time ($t \lesssim 1.0$ ns) difference between the two models can be attributed to these short bending modes. At long times ($t \gtrsim 20$ ns), long-range bending motions present in long chains but absent in a short 10-subunit wlc would produce enhanced bending. Recent triplet anisotropy decay experiments carried out by Hogan et al.[69] on DNA fragments (65–600 base pairs) support the above argument. They concluded that the Barkley and Zimm theory[39] overestimated the decay process for short fragments, but described quite well the decay process for

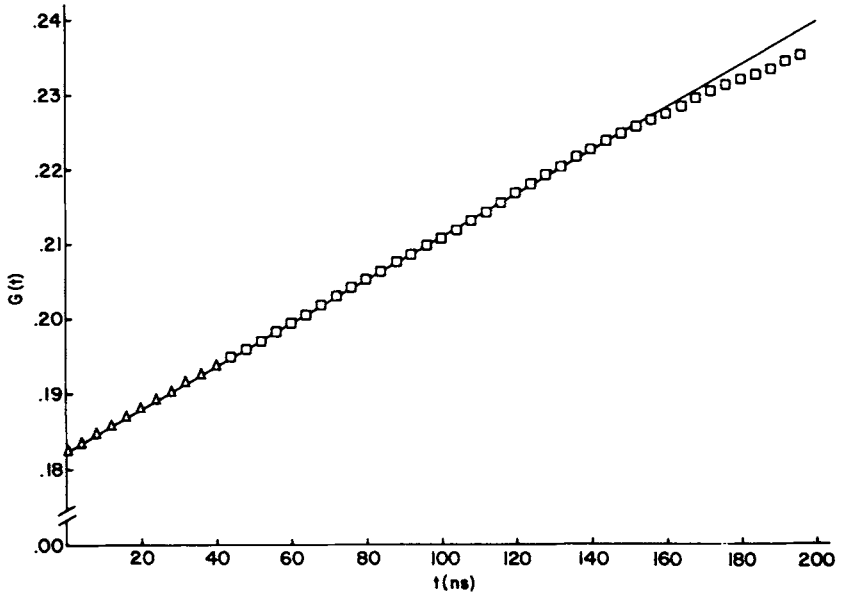

Fig. 5. Light-scattering simulation: p = 600 Å, L = 317.1 Å, Δt (ps) = 100, △; 400, □.

the longest fragment studied. The results of the present simulations are important in connection with fluorescence depolarization studies of DNA torsion and bending,[39,65,69–74] where determination of the torsion elastic constant is complicated by the contribution of bending motions at short times.[74]

Two approximations made in the Barkley and Zimm theory[39] should be pointed out. First, hydrodynamic interaction was accounted for using a straight cylinder rather than a wlc model. Second, tensile forces acting along the chain that would be expected to reduce the amplitudes of the bending motions were ignored. Because of the large persistence length of DNA, the first approximation is undoubtedly a very good one for that particular system. The validity of the second approximation is more difficult to judge. One of the reviewers pointed out that electric birefringence, electric dichroism, and depolarized light scattering experiments on long DNA fragments reveal little internal motion over that assigned to rotations of "persistence lengths" and concludes that bending modes shorter than about 800 Å do not contribute anywhere near the amount of internal motion predicted by the Barkley and Zimm theory.[39] We would like to emphasize, however, that these experiments measure a somewhat different internal average over the motions of the chain than fluorescence depolarization. In fluorescence depolarization, the internal average is $\langle P_2\{\hat{u}(0)\cdot\hat{u}(t)\}\rangle$ where $\hat{u}$ is a unit vector along a single dipole [see Eq. (8)]. In the case of depolarized light scattering, the internal average is $\langle P_2\{\hat{u}_i(0)\cdot\hat{u}_j(t)\}\rangle$ and is summed over all possible dipole combinations, (i,j), in the chain.[75] We

have recently carried out simulations in which the more complex average has been evaluated in addition to the simpler one. *The average for depolarized light scattering, unlike the corresponding average for fluorescence depolarization, turns out to be nearly insensitive to the rapid bending motions.* Hence, the results cited by the reviewer are probably a consequence of the limited resolution of those experiments and not a consequence of the underlying dynamical theory.

Although the results of the light-scattering "experiment" were anticipated from existing theory,[66] it is rather interesting to observe how different experiments probe different dynamic as well as conformational aspects of the same model system. Whereas fluorescence depolarization serves as an extremely sensitive probe to rapid internal rotational motions, light scattering is insensitive to these rapid internal motions and monitors the much slower translational diffusion of the total structure. It should be emphasized, however, that this is only true for low-angle scattering ($qL \lesssim 1$). Light scattering from large macromolecules like DNA reveals considerable internal motion, although it is necessary to interprete these results in terms of simplified bead-spring model parameters at the present time.[31,66,76,77]

In this article, we have reported two dynamic computer "experiments" on a short wormlike chain model. Each complete simulation required 30–90 min of CPU time on an AS9000/N computer, depending on the total number of dynamics steps (200–600 per chain). Since CPU $\sim N^2$ for this model, it would be difficult to extend these studies directly to much longer chain. Nonetheless, we feel that short-chain simulations may serve as a valuable *complement* to analytic theories of long chains, in addition to their direct value in simulating experiments on short chains.

We thank Professor J. M. Schurr for useful discussions. This work was supported in part by NSF and NIH. J.A.M. is an Alfred P. Sloan Fellow, a Camille and Henry Dreyfus Teacher Scholar, and a NIH Research Career Development Awardee.

References

1. Bloomfield, V. A., Crothers, D. M. & Tinoco, I. Jr. (1974) in *Physical Chemistry of the Nucleic Acids*, Harper & Row, New York, Chap. 5.

2. Harvey, S. C. & Cheung, H. C. (1982) in *Muscle and Nonmuscle Motility*, Dowben, R. M. & Shay, J. W., Eds., Plenum, New York.

3. Lowey, S. (1971) in *Subunits in Biological Systems*, Part A, Timasheff, S. N. & Fasman, G. D., Eds., Marcel Dekker, New York, pp. 201–259.

4. Ehrenberg, M., Rigler, R. & Wintermayer, W. (1979) *Biochemistry* **18,** 4588–4599.

5. Yguerabide, J., Epstein, H. F. & Stryer, L. (1970) *J. Mol. Biol.* **51,** 573–590.

6. Holowka, D. A. & Cathou, R. E. (1976) *Biochemistry* **15,** 3379–3390.

7. Timofeev, V. P., Dudich, I. V., Sykulev, Y. K. & Nezlin, R. S. (1978) *FEBS Lett.* **89,** 191–195.

8. Lovejoy, C., Holowka, D. A. & Cathou, R. C. (1977) *Biochemistry* **17,** 3668–3672.

9. Mao, B., Pear, M. R., McCammon, J. A. & Quicho, F. A. (1982) *J. Biol. Chem.* **10,** 1131–1133.

10. McCammon, J. A., Gelin, B. R., Karplus, M. & Wolynes, P. G. (1976) *Nature* **262,** 325–326.
11. McCammon, J. A. & Deutch, J. M. (1976) *Biopolymers* **15,** 1397–1408.
12. Garcia de la Torre, J. & Bloomfield, V. A. (1977) *Biopolymers* **16,** 1747–1763, 1765–1778.
13. Nakajima, H. & Wada, Y. (1977) *Biopolymers* **16,** 875–893.
14. Teller, D. C., Swanson, E. & de Haen, C. (1980) *J. Chem. Phys.* **72,** 1623–1628.
15. Garcia de la Torre, J. & Bloomfield, V. A. (1981) *Q. Rev. Biophys.* **14,** 81–139.
16. Harvey, S. C. (1979) *Biopolymers* **18,** 1081–1104.
17. Harvey, S. C. & Cheung, H. C. (1980) *Biopolymers* **19,** 913–930.
18. Harvey, S. C., Mellado, P. & Garcia de la Torre, J. (1983) *J. Chem. Phys.* **78,** 2081–2090.
19. Wegener, W. A. (1980) *Biopolymers* **19,** 1899–1908.
20. Wegener, W. A., Dowben, R. M. & Koester, V. J. (1980) *J. Chem. Phys.* **73,** 4086–4097.
21. Wegener, W. A. (1982) *Biopolymers* **21,** 1049–1080.
22. Wegener, W. A. (1982) *J. Chem. Phys.* **76,** 6425–6430.
23. Allison, S. A. & McCammon, J. A. (1983) *Biopolymers* **22,** 167–187.
24. Zero, K. & Pecora, R. (1982) *Macromolecules* **15,** 1023–1027.
25. Kirkwood, J. G. (1967) in *Macromolecules*, Auer, P. L., Ed. Gordon and Breach, New York.
26. Zimm, B. H. (1956) *J. Chem. Phys.* **24,** 269–278.
27. Wilson, R. W. & Schellman, J. A. (1977) *Biopolymers* **16,** 2143–2165.
28. Wilson, R. W. & Schellman, J. A. (1978) *Biopolymers* **17,** 1235–1248.
29. Pecora, R. (1965) *J. Chem. Phys.* **43,** 1562–1564.
30. Pecora, R. (1968) *J. Chem. Phys.* **49,** 1036–1043.
31. Lin, S. C. & Schurr, J. M. (1978) *Biopolymers* **17,** 425–461.
32. Zimm, B. H. (1980) *Macromolecules* **13,** 592–602.
33. Wilemski, G. & Tanaka G. (1981) *Macromolecules* **14,** 1531–1538.
34. Fixman, M. (1981) *Macromolecules* **14,** 1706–1709, 1710–1717.
35. Fixman, M. (1983) *J. Chem. Phys.* **78,** 1588–1593, 1594–1599.
36. Harris, R. A. & Hearst, J. E. (1966) *J. Chem. Phys.* **44,** 2595–2602.
37. Fujime, S. & Maruyama, M. (1973) *Macromolecules* **6,** 237–241.
38. Moro, K. & Pecora, R. (1978) *J. Chem. Phys.* **69,** 3254–3261.
39. Barkley, M. D. & Zimm, B. H. (1979) *J. Chem. Phys.* **70,** 2991–3008.
40. Yamakawa, H. & Yoshizaki, T. (1981) *J. Chem. Phys.* **75,** 1016–1030.
41. Yamakawa, H., Yoshizaki, T. & Shimada, J. (1983) *J. Chem. Phys.* **78,** 560–571.
42. Yamakawa, H. & Yoshizaki, T. (1983) *J. Chem. Phys.* **78,** 572–587.
43. Fixman, M. (1978) *J. Chem. Phys.* **69,** 1527–1537, 1538–1545.
44. Helfand, E., Wasserman, Z. R., Weber, T. A., Skolnick, J. & Runnels, J. H. (1981) *J. Chem. Phys.* **75,** 4441–4445.
45. Pear, M. R. & Weiner, J. H. (1979) *J. Chem. Phys.* **71,** 212–224; (1980) **72,** 3939–3947.
46. Levy, R. M., Karplus, M. & McCammon, J. A. (1979) *Chem. Phys. Lett.* **65,** 4–11.
47. Evans, G. T. & Knauss, D. C. (1980) *J. Chem. Phys.* **72,** 1504–1511.
48. McCammon, J. A., Northrup, S. H., Karplus, M. & Levy, R. M. (1980) *Biopolymers* **19,** 2033–2045.
49. Pear, M. R., Northrup, S. H., McCammon, J. A., Karplus, M. & Levy, R. M. (1981) *Biopolymers* **20,** 629–632.
50. McCammon, J. A. & Karplus, M. (1980) *Annu. Rev. Phys. Chem.* **31,** 29–45.
51. Pear, M. R. & McCammon, J. A. (1981) *J. Chem. Phys.* **74,** 6922–6925.
52. Ryckaert, J. P. & Bellemans, A. (1975) *Chem. Phys. Lett.* **30,** 123–125.
53. Weber, T. A. (1978) *J. Chem. Phys.* **69,** 2347–2354; (1979) **70,** 4277–4285.
54. Rossky, P. J. & Karplus, M. (1979) *J. Am. Chem. Soc.* **101,** 1913–1937.
55. Bishop, M., Kalos, M. H. & Frisch, H. L. (1979) *J. Chem. Phys.* **70,** 1299–1304.

56. Rosenberg, R. O. Berne, B. J. & Chandler, D. (1980) *Chem. Phys. Lett.* **75,** 162–168.
57. Gotlib, Y. Y., Balabaev, N. K., Darinskii, A. A. & Neelov, I. M. (1980) *Macromolecules* **13,** 602–608.
58. Ermak, D. L. & McCammon, J. A. (1978) *J. Chem. Phys.* **69,** 1352–1360.
59. Fixman, M. & Kovak, J. (1974) *J. Chem. Phys.* **61,** 4939–4949.
60. Hagerman, P. J. & Zimm, B. H. (1981) *Biopolymers* **20,** 1481–1502.
61. Rotne, J. & Prager, S. (1969) *J. Chem. Phys.* **50,** 4831–4837.
62. Yamakawa, H. (1970) *J. Chem. Phys.* **53,** 436–443.
63. *IMSL Library 7 Reference Manual* (1975) IMSL International and Statistical Libraries, Inc., Houston, Texas.
64. Belford, G. G., Belford, R. L. & Weber, G. (1972) *Proc. Natl. Acad. Sci. USA* **69,** 1392–1393.
65. Schurr, J. M. (1982) *Chem. Phys.* **65,** 417–424.
66. Berne, B. J. & Pecora, R. (1976) *Dynamic Light Scattering*, John Wiley, New York.
67. Allison, S. A., Shibata, J., Wilcoxin, J. & Schurr, J. M. (1982) *Biopolymers* **21,** 729–762.
68. Norisuye, T., Motokowa, M. & Fujita, H. (1979) *Macromolecules* **12,** 320–323.
69. Hogan, M., Wang, J., Austin, R. H., Monitto, C. L. & Hershkowitz, S. (1982) *Proc. Natl. Acad. Sci. USA* **79,** 3518–3522.
70. Wahl, Ph., Paoletti, J. & Le Pecq, J. B. (1970) *Proc. Natl. Acad. Sci. USA* **65,** 417–421.
71. Allison, A. A. & Schurr, J. M. (1979) *Chem. Phys.* **41,** 35–59.
72. Thomas, J. C., Allison, S. A., Appellof, C. J. & Schurr, J. M. (1980) *Biophys. Chem.* **12,** 177–188.
73. Millar, D. P., Robbins, R. J. & Zewail, A. (1980) *Proc. Natl. Acad. Sci. USA* **77,** 5593–5597.
74. Millar, D. P., Robbins, R. J. & Zewail, A. (1982) *J. Chem. Phys.* **76,** 2080–2094.
75. Carpenter, D. K. & Skolnick, J. (1981) *Macromolecules* **14,** 1284–1290.
76. Thomas, J. C., Allison, S. A., Schurr, J. M. & Holder, R. D. (1980) *Biopolymers* **19,** 1451–1474.
77. Kam, Z., Borochov, N. & Eisenberg, H. (1981) *Biopolymers* **20,** 2671–2690.

Received March 28, 1983
Accepted June 15, 1983